

Spontaneous emission of an atom placed near a nanobelt of elliptical cross-section

D.V. Guzatov and V.V. Klimov *

P.N. Lebedev Physical Institute, Russian Academy of Sciences,
53 Leninsky Prospect, 119991 Moscow, Russia

August 15, 2018

Abstract

Spontaneous emission of an atom (molecule) placed near a nanocylinder of elliptical cross-section of an arbitrary composition is studied. The analytical expressions have been obtained for the radiative and nonradiative channels of spontaneous decay and investigated in details.

1 Introduction

As was first pointed out by Purcell [1] one can change the atomic decay rate by using a resonant cavity. It is well known now that not only resonant cavities, but also any material body may exert influence on the spontaneous decay rate [2]. Moreover, control for the spontaneous decay rate is widely used in practice at elaboration of new efficient light sources [3].

Due to rapid development of nanotechnologies influence of nanoparticles of different shapes on radiation of atoms, molecules and nanocrystal quantum dots is of key importance. This direction often referred to as nanophotonics [4]. Influence of spherical [5]-[7], spheroidal [8]-[10] and even ellipsoidal [11] nanoparticle on radiation of atoms and molecules is investigated in details.

Of special interest is the influence of dielectric fibers or metallic wires of different cross-sections on the decay rate of a single atom. This is because the charged wires were employed successfully in order to control the atomic motion [12, 13]. The cylindrical geometry is also important for the investigation of fluorescence of substances in submicron capillaries [14, 15]. A very important application of the decay rate theory in the presence of dielectric fiber had been in the case of the photonic wire lasers [16]-[19]. Finally, the circular cylindrical geometry appears naturally at analysis of the carbon nanotubes [20, 21].

The influence of a perfectly conducting cylindrical surface on decay rates has been well investigated for an atom placed both inside a cylindrical cavity

*vklim@sci.lebedev.ru

[22]-[25] and near a perfectly conducting cylinder [26]. Spontaneous emission of an atom located inside a coaxial waveguide was considered in [27].

The interaction of an atom with a dielectric, semiconductor, or a metallic cylinder is a more complicated process. Van der Waals interaction between an atom and a circular metallic nanowire was considered in [28]. The first investigation of the decay rate of an atom placed at the axis of a circular dielectric fiber was undertaken within a classical approach in [29, 30]. Recently that problem attracted new interest [31]-[36]. In [37, 38] the spontaneous emission near carbon nanotubes was considered.

Recently non-circular nanocylinders (the so called nanobelts or nanoribbons) were successfully synthesized [39]-[43]. Figure 1 illustrates the experimentally obtained nanobelts [39].

The significance of studying such nanoobjects is very great because they form the basis for the synthesis of all kinds of nanodevices, such as nano-scale transducers, actuators, or sensors [44]-[47]. The influence of such structures on optical characteristics of atoms and molecules had not been yet considered, as far as we know.

The aim of this work is to investigate theoretically the influence of dielectric and metallic cylinders of elliptical cross-section on the spontaneous emission of atoms and molecules placed close to the cylinder. This geometry is close to synthesized nanobelts and nanoribbons.

Though it is possible to separate variables in the Helmholtz equation within the elliptic cylinder coordinates, still the electrodynamics and optics of the dielectric elliptic cylinder remain insufficiently studied, due to mathematical difficulties concerned with the Mathieu function [48]. In this paper we shall try to make up for this deficiency, and shall report the investigation results dealing with the spontaneous emission of the atom placed near an infinite elliptic cylinder.

Some elements of the theory for a spontaneous decay of an atom near material bodies will be presented in section 2, where the main attention will be paid to the nanobodies, whose dimensions are small as compared to the radiation wavelength. In section 3, we report solution on a problem of spontaneous decay of an atom near the perfectly conducting elliptic cylinder with arbitrarily sized cross-section when retardation effects can be important. In section 4, the radiative and nonradiative channels of a decaying atom located near an elliptic nanocylinder, which is made of an arbitrary material, will be considered analytically within the quasistatic approach. The results obtained in sections 3 and 4 will be analyzed and illustrated graphically in section 5. The geometry of the problem under study is illustrated in Fig.2.

2 Some elements of the theory for the spontaneous emission of an atom placed near the nanobodies

At weak coupling of an atom and a nanobody, i.e. in the case of the exponential spontaneous decay, the expression for the linewidth γ_a of excited level a has the form [49]:

$$\gamma_a = \gamma_{a,0} + \frac{2}{\hbar} \sum_n \sum_{\alpha,\beta=1}^3 d_{0,\alpha}^{an} d_{0,\beta}^{na} \text{Im} \{G_{\alpha\beta}(\mathbf{r}', \mathbf{r}'; \omega_{na})\} \Theta(\omega_{an}) \quad (1)$$

where $\gamma_{a,0}$ is the linewidth in free space without nanobodies; $d_{0,\alpha}^{an}$, the matrix element of the dipole moment operator between the states a and n ; $\omega_{an} = (W_a - W_n)/\hbar$; and $G_{\alpha\beta}$, the reflected part of the classical Green's function connected with the reflected field E_α^r of a dipole \mathbf{d}_0^{na} is placed at point \mathbf{r}' by the relation

$$E_\alpha^r(\mathbf{r}) = \sum_{\beta=1}^3 d_{0,\beta}^{na} G_{\alpha\beta}(\mathbf{r}, \mathbf{r}'; \omega_{na}) \quad (2)$$

In Eqs. (1) and (2), $\alpha, \beta = 1, 2, 3$ are the indices of the Cartesian axes, and Θ is the Heaviside's unit-step function. Note that Eq.(1) has been obtained within the framework of the most general assumptions (Fermi's golden rule and the fluctuation-dissipation theorem), and has a very large domain of applicability. From Eq.(1) it is seen that total linewidth is the sum of partial widths, and below we shall consider, for simplicity, the rate of transitions between some two states only.

In the case of the nanobodies one can use the Rayleigh's perturbation long wavelength theory. The Green's function of the reflected field may be represented as the power series in the wave vector [50]:

$$G_{\alpha\beta}(\mathbf{r}, \mathbf{r}'; \omega) = G_{\alpha\beta}^{(0)}(\mathbf{r}, \mathbf{r}') + k G_{\alpha\beta}^{(1)}(\mathbf{r}, \mathbf{r}') + k^2 G_{\alpha\beta}^{(2)}(\mathbf{r}, \mathbf{r}') + ik^3 G_{\alpha\beta}^{(3)}(\mathbf{r}, \mathbf{r}') + \dots \quad (3)$$

where $G_{\alpha\beta}^{(j)}$ ($j=0, 1, 2, \dots$) are the coefficients that can be found from a solution of the corresponding quasistatic problems; $k = \omega/c$. The first three terms (3) describe the near fields, while the radiation fields emerge starting from the 4th term. By substituting Eq.(3) into (1) for the total rate of spontaneous decay $\gamma_{e \rightarrow g}$ from the state e into g near the nanobody, we obtain the following expression:

$$\begin{aligned}
\gamma_{e \rightarrow g} = & \underbrace{\frac{2}{\hbar} \sum_{\alpha, \beta=1}^3 d_{0,\alpha}^{eg} d_{0,\beta}^{ge} \text{Im} \left\{ G_{\alpha\beta}^{(0)}(\mathbf{r}', \mathbf{r}') + \dots \right\}}_{\text{nonradiative}} \\
& + \underbrace{\gamma_{0,e \rightarrow g} + \frac{2}{\hbar} \sum_{\alpha, \beta=1}^3 d_{0,\alpha}^{eg} d_{0,\beta}^{ge} \text{Re} \left\{ k^3 G_{\alpha\beta}^{(3)}(\mathbf{r}', \mathbf{r}') + \dots \right\}}_{\text{radiative}} \quad (4)
\end{aligned}$$

Here $k \approx \omega_0/c$, and γ_0 and ω_0 are unperturbed by a nanobody the rate and frequency of transitions between the states a and g . The first term of Eq.(4) is nonzero for the absorbing media only, whereas the rest of the terms are nonzero in the absence of absorption as well (the dielectric or the perfectly conducting nanobodies). Those terms describe mostly the radiative losses. Thus, to determine the main terms of the nonradiative and radiative losses it is necessary to determine $G_{\alpha\beta}^{(0)}(\mathbf{r}', \mathbf{r}')$ and $G_{\alpha\beta}^{(3)}(\mathbf{r}', \mathbf{r}')$, respectively.

It is a complex problem to determine directly the radiative losses described by the 3-d order terms by k . But in the case of an atom localized close to a nanobody the radiation is dipole-like, and the total dipole moment of the atom + nanobody system could be found from $G_{\alpha\beta}^{(0)}(\mathbf{r}, \mathbf{r}')$ at large distances from the system. Thus, in the case of the nanobodies the radiative rate of the spontaneous transition (the transition from e into g) will be described by [35]:

$$\frac{\gamma^{radiative}}{\gamma_0} = \frac{|\mathbf{d}_0 + \delta\mathbf{d}|^2}{d_0^2}, \quad (5)$$

where $\mathbf{d}_{total} = \mathbf{d}_0 + \delta\mathbf{d}$ is the total dipole moment of the atom + nanobody system, and $\delta\mathbf{d}$ is the dipole moment induced in the nanobody. Here we will omit superscript eg in transition dipole moment \mathbf{d}_0^{eg} and in $\gamma_{e \rightarrow g}$ and $\gamma_{0,e \rightarrow g}$.

It should be noted that beside the radiative and nonradiative channels of the spontaneous decay for a dielectric cylinder (and for any dielectric waveguided structure) one must take into account energy transfer into the waveguided modes. In case of the dielectric (nonmetallic) nanobodies that correction is exponentially small [35] and may be neglected. But in case of the complex dielectric permittivity of a nanocylinder (real metals), the spontaneous decay waveguiding rate may be no longer a small value, and that correction should be taken into account.

Thus, to describe the decay rate of an atom in the presence of a nanobody one should determine the reflected field \mathbf{E}^r in a quasistatic approximation, and the dipole moment $\delta\mathbf{d}$ induced in the nanobody. For a nanocylinder which size is comparable with radiation wavelength one should use full set of Maxwell's equations to find the reflected field.

3 Spontaneous decay rate of an atom near a perfectly conducting elliptic cylinder

The problem of the spontaneous atomic decay near a perfectly conducting elliptic cylinder of any geometry may be solved analytically in the elliptic cylinder coordinates (Fig.3) ($1 \leq u < \infty$, $-1 \leq v \leq 1$, $-\infty < z < \infty$) [48]

$$x = fuv, \quad y = f\sqrt{(u^2 - 1)(1 - v^2)}, \quad z = z, \quad (6)$$

where $f = \sqrt{a^2 - b^2}$ is the half-distance between the cylinder foci. Expression $u = u_0 = a/f$ specifies the surface of the studied cylinder.

Total field from the arbitrary current $\mathbf{j}(\mathbf{r})$ and charge $\rho(\mathbf{r})$ densities near the perfectly conducting elliptic cylinder can be found from the equations [51, 52]

$$\begin{aligned} E_z^{TM}(\mathbf{r}) &= \int dr' \left(ik \frac{j_z(\mathbf{r}')}{c} + \rho(\mathbf{r}') \frac{\partial}{\partial z'} \right) G^{TM}(\mathbf{r}, \mathbf{r}'), \\ H_z^{TE}(\mathbf{r}) &= \frac{1}{c} \int dr' [\mathbf{j}(\mathbf{r}') \times \nabla']_z G^{TE}(\mathbf{r}, \mathbf{r}'), \end{aligned} \quad (7)$$

where the electric and magnetic Green's functions G^{TM} and G^{TE} are of the following form [51] ($u > u' > u_0$)

$$\begin{aligned} G^{TM}(\mathbf{r}, \mathbf{r}') &= 2i \sum_{\sigma=e,o} \sum_{n=0}^{\infty} \int d\alpha e^{i\alpha(z-z')} \frac{S\sigma_n(\beta f, v) S\sigma_n(\beta f, v')}{M\sigma_n(\beta f)} \\ &\quad \times H^{(1)}\sigma_n(\beta f, u) \left(J\sigma_n(\beta f, u') - H^{(1)}\sigma_n(\beta f, u') \right. \\ &\quad \left. \times \frac{J\sigma_n(\beta f, u_0)}{H^{(1)}\sigma_n(\beta f, u_0)} \right), \end{aligned} \quad (8)$$

$$\begin{aligned} G^{TE}(\mathbf{r}, \mathbf{r}') &= 2i \sum_{\sigma=e,o} \sum_{n=0}^{\infty} \int d\alpha e^{i\alpha(z-z')} \frac{S\sigma_n(\beta f, v) S\sigma_n(\beta f, v')}{M\sigma_n(\beta f)} \\ &\quad \times H^{(1)}\sigma_n(\beta f, u) \left(J\sigma_n(\beta f, u') - H^{(1)}\sigma_n(\beta f, u') \right. \\ &\quad \left. \times \frac{(\partial/\partial w) J\sigma_n(\beta f, w)}{(\partial/\partial w) H^{(1)}\sigma_n(\beta f, w)} \Big|_{w=u_0} \right), \end{aligned} \quad (9)$$

where $\beta = (k^2 - \alpha^2)^{1/2}$; $S\sigma_n$ denote the ‘‘angular’’ even ($\sigma = e$) and odd ($\sigma = o$) Mathieu functions defined as follows [48]:

$$\begin{aligned}
Se_{2n}(h, \cos \theta) &= \sum_{m=0}^{\infty} Be_{2n}^{2m}(h) \cos(2m\theta), \\
Se_{2n+1}(h, \cos \theta) &= \sum_{m=0}^{\infty} Be_{2n+1}^{2m+1}(h) \cos((2m+1)\theta), \\
So_{2n+1}(h, \cos \theta) &= \sum_{m=0}^{\infty} Bo_{2n+1}^{2m+1}(h) \sin((2m+1)\theta), \\
So_{2n}(h, \cos \theta) &= \sum_{m=1}^{\infty} Bo_{2n}^{2m}(h) \sin(2m\theta), \tag{10}
\end{aligned}$$

where $B\sigma_n^m(h)$ are the expansion coefficients ($Bo_0^{2m}(h) = 0$); $J\sigma_n$ and $H^{(1)}\sigma_n$ are the ‘‘radial’’ Mathieu functions, which are expressed through the same coefficients $B\sigma_n^m(h)$. For example, functions $J\sigma_n$ can be written down as [48]:

$$\begin{aligned}
Je_{2n}(h, u) &= \sqrt{\frac{\pi}{2}} \sum_{m=0}^{\infty} (-1)^{n-m} Be_{2n}^{2m}(h) J_{2m}(hu), \\
Je_{2n+1}(h, u) &= \sqrt{\frac{\pi}{2}} \sum_{m=0}^{\infty} (-1)^{n-m} Be_{2n+1}^{2m+1}(h) J_{2m+1}(hu), \\
Jo_{2n+1}(h, u) &= \sqrt{\frac{\pi}{2}} \frac{\sqrt{u^2-1}}{u} \\
&\quad \times \sum_{m=0}^{\infty} (-1)^{n-m} (2m+1) Bo_{2n+1}^{2m+1}(h) J_{2m+1}(hu), \\
Jo_{2n}(h, u) &= \sqrt{\frac{\pi}{2}} \frac{\sqrt{u^2-1}}{u} \sum_{m=1}^{\infty} (-1)^{n-m} 2m Bo_{2n}^{2m}(h) J_{2m}(hu), \tag{11}
\end{aligned}$$

where J_n are the Bessel functions. For the functions $H^{(1)}\sigma_n$ the analogous expansions will be valid provided that the Hankel functions are used (substitute $J_m \rightarrow H_m^{(1)}$ in Eq.(11)). The normalization constant $M\sigma_n(h)$ is determined by the expression $M\sigma_n(h) = \int_0^{2\pi} d\theta [S\sigma_n(h, \cos \theta)]^2$.

Integration over the longitudinal wave number α in Eqs. (8) and (9) is performed along the real axis assuming that the wave number k has a positive infinitely small imaginary addition ($k \rightarrow k + i0^+$). It should also be noted that the first part of Eqs. (8) and (9) (which is proportional to $J\sigma_n(f\beta, u')$) corresponds to Green’s function for free space (in the absence of a cylinder), whereas the second part (which is proportional to $H^{(1)}\sigma_n(f\beta, u')$) corresponds to the reflected field.

Note also that for a near-circular cylinder ($f \rightarrow 0$) one can obtain from Eqs. (8) and (9) the respective expressions for the Green’s functions in cylindrical coordinates (ρ, φ) if we set that

$$\begin{aligned}
\frac{S e_n(f\beta, v)}{\sqrt{M e_n(f\beta)}} J e_n(f\beta, u) &\rightarrow \frac{\cos(n\varphi)}{\sqrt{2(1+\delta_{0,n})}} J_n(\beta\rho), \\
\frac{S o_n(f\beta, v)}{\sqrt{M o_n(f\beta)}} J o_n(f\beta, u) &\rightarrow \frac{\sin(n\varphi)}{\sqrt{2}} J_n(\beta\rho),
\end{aligned} \tag{12}$$

where $\delta_{0,n}$ is Kronecker's δ -symbol. Analogous expressions for the functions $H^{(1)}\sigma_n$ are obtained from (12) via a substitution $J_n \rightarrow H_n^{(1)}$.

The charge and current densities at excitation by a point dipole (atom) have the form:

$$\begin{aligned}
\rho &= -(\mathbf{d}_0 \nabla) \delta(\mathbf{r}-\mathbf{r}') e^{-i\omega t}, \\
j &= -i\omega d_0 \delta(\mathbf{r}-\mathbf{r}') e^{-i\omega t},
\end{aligned} \tag{13}$$

where \mathbf{d}_0 is the transition dipole moment (below just the dipole moment) of an atom placed at point \mathbf{r}' (below, the primed coordinates will denote the atomic position). The exponential term $e^{-i\omega t}$ will be omitted.

Knowing the field components (7) we shall determine the rest of the field components both for TM and TE modes [53]

$$\begin{aligned}
E_{u,\alpha}^{TM} &= \frac{i\alpha}{\beta^2 f} \sqrt{\frac{u^2-1}{u^2-v^2}} \frac{\partial E_{z,\alpha}^{TM}}{\partial u}, & E_{v,\alpha}^{TM} &= \frac{i\alpha}{\beta^2 f} \sqrt{\frac{1-v^2}{u^2-v^2}} \frac{\partial E_{z,\alpha}^{TM}}{\partial v}, \\
E_{u,\alpha}^{TE} &= -\frac{ik}{\beta^2 f} \sqrt{\frac{1-v^2}{u^2-v^2}} \frac{\partial H_{z,\alpha}^{TE}}{\partial v}, & E_{v,\alpha}^{TE} &= \frac{ik}{\beta^2 f} \sqrt{\frac{u^2-1}{u^2-v^2}} \frac{\partial H_{z,\alpha}^{TE}}{\partial u}.
\end{aligned} \tag{14}$$

In Eq.(14) the α index denotes the respective Fourier transform for the z coordinate. Total field is the sum of the TE and TM field components.

In the case of the dipole source (13), the expressions (7) for the fields may be rewritten in the following form:

$$\begin{aligned}
E_z^{TM}(\mathbf{r}) &= k^2 d_{0,z} G^{TM}(\mathbf{r}, \mathbf{r}') + (\mathbf{d}_0 \nabla') \frac{\partial}{\partial z'} G^{TM}(\mathbf{r}, \mathbf{r}'), \\
H_z^{TE}(\mathbf{r}) &= -ik [\mathbf{d}_0 \times \nabla']_z G^{TE}(\mathbf{r}, \mathbf{r}').
\end{aligned} \tag{15}$$

By using (8), (9), and (14), (15) one can represent the spontaneous emission rate (1) as the sum of the TM and TE contributions:

$$\frac{\gamma}{\gamma_0} = 1 - \frac{3}{2} \text{Re}(W^{TM} + W^{TE}). \tag{16}$$

In some particular cases Eq.(16) will take the next relatively simple form.

Dipole moment is oriented along x-axis ($\mathbf{d}_0 = d_0 \mathbf{e}_x$)

A) Atom is placed on the x -axis ($\mathbf{r}' = x'\mathbf{e}_x$)

$$W_x^{TM} = 4 \sum_{n=0}^{\infty} \int_0^k d\alpha \frac{\alpha^2}{k^3 (\beta f)^2} \frac{1}{M e_n(\beta f)} \times \left[\frac{\partial}{\partial u'} H^{(1)} e_n(\beta f, u') \right]^2 \frac{J e_n(\beta f, u_0)}{H^{(1)} e_n(\beta f, u_0)}, \quad (17)$$

$$W_x^{TE} = \frac{4}{u'^2 - 1} \sum_{n=0}^{\infty} \int_0^k \frac{d\alpha}{k (\beta f)^2} \frac{1}{M o_n(\beta f)} \times \left[H^{(1)} o_n(\beta f, u') \right]^2 \frac{(\partial/\partial w) J o_n(\beta f, w)}{(\partial/\partial w) H^{(1)} o_n(\beta f, w)} \Big|_{w=u_0}. \quad (18)$$

B) Atom is placed on the y -axis ($\mathbf{r}' = y'\mathbf{e}_y$)

$$W_x^{TM} = \frac{4}{u'^2} \sum_{n=0}^{\infty} \int_0^k d\alpha \frac{\alpha^2}{k^3 (\beta f)^2} \frac{[(\partial/\partial v') S e_{2n+1}(\beta f, v')|_{v'=0}]^2}{M e_{2n+1}(\beta f)} \times \left[H^{(1)} e_{2n+1}(\beta f, u') \right]^2 \frac{J e_{2n+1}(\beta f, u_0)}{H^{(1)} e_{2n+1}(\beta f, u_0)} + \frac{4}{u'^2} \sum_{n=0}^{\infty} \int_0^k d\alpha \frac{\alpha^2}{k^3 (\beta f)^2} \frac{[(\partial/\partial v') S o_{2n}(\beta f, v')|_{v'=0}]^2}{M o_{2n}(\beta f)} \times \left[H^{(1)} o_{2n}(\beta f, u') \right]^2 \frac{J o_{2n}(\beta f, u_0)}{H^{(1)} o_{2n}(\beta f, u_0)}, \quad (19)$$

$$W_x^{TE} = 4 \left(1 - \frac{1}{u'^2} \right) \sum_{n=0}^{\infty} \int_0^k \frac{d\alpha}{k (\beta f)^2} \frac{[S e_{2n}(\beta f, 0)]^2}{M e_{2n}(\beta f)} \times \left[\frac{\partial}{\partial u'} H^{(1)} e_{2n}(\beta f, u') \right]^2 \frac{(\partial/\partial w) J e_{2n}(\beta f, w)}{(\partial/\partial w) H^{(1)} e_{2n}(\beta f, w)} \Big|_{w=u_0} + 4 \left(1 - \frac{1}{u'^2} \right) \sum_{n=0}^{\infty} \int_0^k \frac{d\alpha}{k (\beta f)^2} \frac{[S o_{2n+1}(\beta f, 0)]^2}{M o_{2n+1}(\beta f)} \times \left[\frac{\partial}{\partial u'} H^{(1)} o_{2n+1}(\beta f, u') \right]^2 \frac{(\partial/\partial w) J o_{2n+1}(\beta f, w)}{(\partial/\partial w) H^{(1)} o_{2n+1}(\beta f, w)} \Big|_{w=u_0} \quad (20)$$

Dipole moment is oriented along y -axis ($\mathbf{d}_0 = d_0 \mathbf{e}_y$)

A) Atom is placed on the x-axis ($\mathbf{r}' = x' \mathbf{e}_x$)

$$W_y^{TM} = \frac{4}{u'^2 - 1} \sum_{n=0}^{\infty} \int_0^k d\alpha \frac{\alpha^2}{k^3 (\beta f)^2} \frac{1}{Mo_n(\beta f)} \times \left[H^{(1)} o_n(\beta f, u') \right]^2 \frac{Jo_n(\beta f, u_0)}{H^{(1)} o_n(\beta f, u_0)}, \quad (21)$$

$$W_y^{TE} = 4 \sum_{n=0}^{\infty} \int_0^k \frac{d\alpha}{k (\beta f)^2} \frac{1}{Me_n(\beta f)} \times \left[\frac{\partial}{\partial u'} H^{(1)} e_n(\beta f, u') \right]^2 \times \frac{(\partial/\partial w) Je_n(\beta f, w)}{(\partial/\partial w) H^{(1)} e_n(\beta f, w)} \Big|_{w=u_0}. \quad (22)$$

B) Atom is placed on the y-axis ($\mathbf{r}' = y' \mathbf{e}_y$)

$$W_y^{TM} = 4 \left(1 - \frac{1}{u'^2} \right) \sum_{n=0}^{\infty} \int_0^k d\alpha \frac{\alpha^2}{k^3 (\beta f)^2} \frac{[Se_{2n}(\beta f, 0)]^2}{Me_{2n}(\beta f)} \times \left[\frac{\partial}{\partial u'} H^{(1)} e_{2n}(\beta f, u') \right]^2 \frac{Je_{2n}(\beta f, u_0)}{H^{(1)} e_{2n}(\beta f, u_0)} + 4 \left(1 - \frac{1}{u'^2} \right) \sum_{n=0}^{\infty} \int_0^k d\alpha \frac{\alpha^2}{k^3 (\beta f)^2} \frac{[So_{2n+1}(\beta f, 0)]^2}{Mo_{2n+1}(\beta f)} \times \left[\frac{\partial}{\partial u'} H^{(1)} o_{2n+1}(\beta f, u') \right]^2 \frac{Jo_{2n+1}(\beta f, u_0)}{H^{(1)} o_{2n+1}(\beta f, u_0)}, \quad (23)$$

$$W_y^{TE} = \frac{4}{u'^2} \sum_{n=0}^{\infty} \int_0^k \frac{d\alpha}{k (\beta f)^2} \frac{[(\partial/\partial v') Se_{2n+1}(\beta f, v')|_{v'=0}]^2}{Me_{2n+1}(\beta f)} \times \left[H^{(1)} e_{2n+1}(\beta f, u') \right]^2 \frac{(\partial/\partial w) Je_{2n+1}(\beta f, w)}{(\partial/\partial w) H^{(1)} e_{2n+1}(\beta f, w)} \Big|_{w=u_0} + \frac{4}{u'^2} \sum_{n=0}^{\infty} \int_0^k \frac{d\alpha}{k (\beta f)^2} \frac{[(\partial/\partial v') So_{2n}(\beta f, v')|_{v'=0}]^2}{Mo_{2n}(\beta f)} \times \left[H^{(1)} o_{2n}(\beta f, u') \right]^2 \frac{(\partial/\partial w) Jo_{2n}(\beta f, w)}{(\partial/\partial w) H^{(1)} o_{2n}(\beta f, w)} \Big|_{w=u_0}. \quad (24)$$

Dipole moment is oriented along z-axis ($\mathbf{d}_0 = d_0 \mathbf{e}_z$)

A) Atom is placed on the x -axis ($\mathbf{r}' = x' \mathbf{e}_x$)

$$W_z^{TM} = 4 \sum_{n=0}^{\infty} \int_0^k d\alpha \frac{\beta^2}{k^3} \frac{1}{Me_n(\beta f)} \left[H^{(1)} e_n(\beta f, u') \right]^2 \frac{Je_n(\beta f, u_0)}{H^{(1)} e_n(\beta f, u_0)},$$

$$W_z^{TE} = 0. \quad (25)$$

B) Atom is placed on the y -axis ($\mathbf{r}' = y' \mathbf{e}_y$)

$$W_z^{TM} = 4 \sum_{n=0}^{\infty} \int_0^k d\alpha \frac{\beta^2}{k^3} \frac{[Se_{2n}(\beta f, 0)]^2}{Me_{2n}(\beta f)} \left[H^{(1)} e_{2n}(\beta f, u') \right]^2 \frac{Je_{2n}(\beta f, u_0)}{H^{(1)} e_{2n}(\beta f, u_0)}$$

$$+ 4 \sum_{n=0}^{\infty} \int_0^k d\alpha \frac{\beta^2}{k^3} \frac{[So_{2n+1}(\beta f, 0)]^2}{Mo_{2n+1}(\beta f)} \left[H^{(1)} o_{2n+1}(\beta f, u') \right]^2$$

$$\times \frac{Jo_{2n+1}(\beta f, u_0)}{H^{(1)} o_{2n+1}(\beta f, u_0)},$$

$$W_z^{TE} = 0. \quad (26)$$

Case of low ellipticity ($f \rightarrow 0$)

If a cylinder has low ellipticity ($f \rightarrow 0$) one can find explicit expressions for the spontaneous emission rate (16) in the form of the power series f . That can be done if the expansion for the coefficients $B\sigma_n^m(h)$ at $h \rightarrow 0$ is known. Keeping the terms of the second-order smallness by h one can write down the expressions for $B\sigma_n^m(h \rightarrow 0)$ in the following form ($n = 1, 2, 3, \dots$):

$$Be_0^0 \approx 1 + \frac{h^2}{8}, \quad Be_0^2 \approx -\frac{h^2}{8},$$

$$Be_{2n}^{2(n-1)} \approx \frac{h^2}{16(2n-1)}, \quad Be_{2n}^{2n} \approx 1 - \frac{h^2}{8(4n^2-1)},$$

$$Be_{2n}^{2(n+1)} \approx -\frac{h^2}{16(2n+1)}, \quad (27)$$

$$Be_1^1 \approx 1 + \frac{h^2}{32}, \quad Be_1^3 \approx -\frac{h^2}{32},$$

$$Be_{2n+1}^{2n-1} \approx \frac{h^2}{32n}, \quad Be_{2n+1}^{2n+1} \approx 1 - \frac{h^2}{32n(n+1)},$$

$$Be_{2n+1}^{2n+3} \approx -\frac{h^2}{32(n+1)}, \quad (28)$$

and

$$\begin{aligned}
Bo_1^1 &\approx 1 + \frac{3h^2}{32}, & Bo_1^3 &\approx -\frac{h^2}{32}, \\
Bo_{2n+1}^{2n-1} &\approx \frac{h^2}{32n(2n+1)}, & Bo_{2n+1}^{2n+1} &\approx \frac{1}{2n+1} \left(1 + \frac{h^2}{32n(n+1)} \right), \\
Bo_{2n+1}^{2n+3} &\approx -\frac{h^2}{32(n+1)(2n+1)},
\end{aligned} \tag{29}$$

$$\begin{aligned}
Bo_{2n}^{2(n-1)} &\approx \frac{h^2}{32n(2n-1)}, & Bo_{2n}^{2n} &\approx \frac{1}{2n} \left(1 + \frac{h^2}{8(4n^2-1)} \right), \\
Bo_{2n}^{2(n+1)} &\approx -\frac{h^2}{32n(2n+1)}.
\end{aligned} \tag{30}$$

The rest of the coefficients Be_n^m are either zero or have a higher infinitesimal order. By substituting Eqs. (27)-(30) into (10) and (11), and assuming that in the cylindrical coordinates (ρ, φ) we have $fu \approx \rho \left(1 + \frac{1}{2} \left(\frac{f}{\rho} \right)^2 \sin^2 \varphi \right)$ and $v \approx \cos \varphi \left(1 - \frac{1}{2} \left(\frac{f}{\rho} \right)^2 \sin^2 \varphi \right)$, we can find expansions in the region of $f \rightarrow 0$ for the Mathieu functions and their derivatives with accuracy up to f^2 . By restricting ourselves to the main expansion terms only, and assuming that $fu' = \rho'$ and $fu_0 = a$ we obtain the following expressions for W^{TM} and W^{TE} .

A) Dipole moment is oriented along ρ -coordinate line

$$\begin{aligned}
W_\rho^{TM} &\approx \sum_{n=0}^{\infty} (2 - \delta_{0,n}) \int_0^k d\alpha \frac{\alpha^2}{k^3} \left[\frac{d}{dz} H_n^{(1)}(z) \Big|_{z=\beta\rho'} \right]^2 \frac{J_n(\beta a)}{H_n^{(1)}(\beta a)} + O(f^2), \\
W_\rho^{TE} &\approx 2 \sum_{n=1}^{\infty} n^2 \int_0^k \frac{d\alpha}{k(\beta\rho')^2} \left[H_n^{(1)}(\beta\rho') \right]^2 \frac{(d/dz) J_n(z)}{(d/dz) H_n^{(1)}(z)} \Big|_{z=\beta a} \\
&\quad + O(f^2).
\end{aligned} \tag{31}$$

B) Dipole moment is oriented along φ -coordinate line

$$\begin{aligned}
W_\varphi^{TM} &\approx 2 \sum_{n=1}^{\infty} n^2 \int_0^k d\alpha \frac{\alpha^2}{k^3(\beta\rho')^2} \left[H_n^{(1)}(\beta\rho') \right]^2 \frac{J_n(\beta a)}{H_n^{(1)}(\beta a)} + O(f^2), \\
W_\varphi^{TE} &\approx \sum_{n=0}^{\infty} (2 - \delta_{0,n}) \int_0^k \frac{d\alpha}{k} \left[\frac{d}{dz} H_n^{(1)}(z) \Big|_{z=\beta\rho'} \right]^2 \\
&\quad \times \frac{(d/dz) J_n(z)}{(d/dz) H_n^{(1)}(z)} \Big|_{z=\beta a} + O(f^2).
\end{aligned} \tag{32}$$

C) Dipole moment is oriented along z -axis

$$\begin{aligned}
W_z^{TM} &\approx \sum_{n=0}^{\infty} (2 - \delta_{0,n}) \int_0^k d\alpha \frac{\beta^2}{k^3} \left[H_n^{(1)}(\beta\rho') \right]^2 \frac{J_n(\beta a)}{H_n^{(1)}(\beta a)} + O(f^2), \\
W_z^{TE} &= 0.
\end{aligned} \tag{33}$$

Note that the main terms (31)-(33) coincide as in the case of the analogous expressions for W_ρ , W_φ , and W_z in the circular cylinder of a radius [26]. This circumstance supports the validity of our calculations.

Atom is placed in close proximity to surface of a cylinder

In the most interesting case of an atom placed in close proximity to the surface of a cylinder ($u' \rightarrow u_0$). The decay rate of a tangentially to surface oriented dipole tends to zero. The nonzero rate of decays is possible if the dipole moment orientation is normal to the cylindrical surface, i.e. for the dipole that is oriented along the u -coordinate line

$$\begin{aligned}
W_u^{TM} &= 4 \left(\frac{u_0^2 - 1}{u_0^2 - v'^2} \right) \sum_{\sigma=e,o} \sum_{n=0}^{\infty} \int_0^k d\alpha \frac{\alpha^2}{k^3 (\beta f)^2} \frac{[S\sigma_n(\beta f, v')]^2}{M\sigma_n(\beta f)} \\
&\quad \times \left[\frac{\partial}{\partial u'} H^{(1)} \sigma_n(\beta f, u') \Big|_{u'=u_0} \right]^2 \frac{J\sigma_n(\beta f, u_0)}{H^{(1)} \sigma_n(\beta f, u_0)}, \\
W_u^{TE} &= 4 \left(\frac{1 - v'^2}{u_0^2 - v'^2} \right) \sum_{\sigma=e,o} \sum_{n=0}^{\infty} \int_0^k \frac{d\alpha}{k (\beta f)^2} \frac{[(\partial/\partial v') S\sigma_n(\beta f, v')]^2}{M\sigma_n(\beta f)} \\
&\quad \times \left[H^{(1)} \sigma_n(\beta f, u_0) \right]^2 \frac{(\partial/\partial w) J\sigma_n(\beta f, w)}{(\partial/\partial w) H^{(1)} \sigma_n(\beta f, w)} \Big|_{w=u_0}.
\end{aligned} \tag{34}$$

When elliptic cylinder radius is tending to zero $kfu_0 \rightarrow 0$, the decay rate (34) of a tangentially to surface oriented dipole tends to zero the main contribution to the decay rates of normally oriented dipole is due to the terms with $n = 0$ and $n = 1$ of (34). By expanding the expressions (10) and (11) into series at kf , $kfu_0 \rightarrow 0$ (the procedure of finding the expansions for the coefficients $B\sigma_0^m$ and $B\sigma_1^m$ is described in detail in [48]) one can obtain from (16) and (34) the next simple asymptotic formula:

$$\begin{aligned}
\left(\frac{\gamma}{\gamma_0}\right)_{u \Big|_{kf u' = kf u_0 \rightarrow 0}} &= \frac{3}{2(u_0^2 - v'^2)(kf)^2} \\
&\times \left(1 + \frac{2}{\pi} \arctan L^*(u_0) + \frac{4(\ln 2 - 1)}{\pi^2(1 + L^{*2}(u_0))} + \dots\right) \\
&+ \frac{(u_0 + \sqrt{u_0^2 - 1})^2}{u_0^2 - v'^2} + \dots
\end{aligned} \tag{35}$$

in which

$$L^*(u_0) = \frac{2}{\pi} \left\{ \ln \left[\frac{kf}{4} \left(u_0 + \sqrt{u_0^2 - 1} \right) \right] + \gamma_E \right\}, \tag{36}$$

where $\gamma_E \approx 0.57722$ is the Euler's constant. In a particular case of a circular cylinder of a -radius ($f \rightarrow 0$, $f u_0 = a$) we obtain from (35) the expansion that coincides with analogous asymptotic expression for the circular cylinder [26]

$$\left(\frac{\gamma}{\gamma_0}\right)_{\rho \Big|_{k\rho' = ka \rightarrow 0}} = \frac{3}{2(ka)^2} \left(1 + \frac{2}{\pi} \arctan L^* + \frac{4(\ln 2 - 1)}{\pi^2(1 + L^{*2})} + \dots\right) + 4 + \dots \tag{37}$$

where $L^* = \frac{2}{\pi} \left[\ln \left(\frac{ka}{2} \right) + \gamma_E \right]$.

In the most interesting case of a very thin nanobelt ($u_0 \rightarrow 1$) the decay rate of the atom (having normal orientation of the dipole moment) can tend both to infinity (the atom is at the nanobelt edge ($v' = \pm 1$)) and take finite values at other positions of the atom. This signifies nontrivial character of the found expressions (35).

4 Spontaneous decay rate of an atom near elliptic nanocylinder made of arbitrary material

In the case of the dielectric or metallic cylinder of arbitrary dimensions and arbitrary permittivity ε the problem of the spontaneous decay rate of an atom may also be solved analytically [54]. But such a solution is so cumbersome that it is very difficult to use it practically. In this section we restrict ourselves to a practically important case of a nanofiber or a metal nanowire of elliptical cross-section. It may be easy to describe the spontaneous decay, in this case.

4.1 The rate of the radiative decays

In order to find the spontaneous radiative decay rate of an atom placed at point \mathbf{r}' near to elliptic nanocylinder of arbitrary material it is necessary to calculate a dipole moment induced in a nanocylinder, in accordance with Eq.(5). In order to

find the dipole moment one may use the found analytical solution [11] for three-axis ellipsoid and turn one of the semi-axes to the infinity (without using the elliptic cylinder coordinates). As a result, the expression for the induced dipole moment on the elliptic cylinder made of material with the dielectric constant ε with semi-axes a and b on the x - and y -axes, respectively (Fig.2), will take the form:

$$\begin{aligned} \delta \mathbf{d} = & -\frac{3}{2} (d_{0,x} P_{xx} F_a(\xi') \mathbf{e}_x + d_{0,y} P_{yy} F_b(\xi') \mathbf{e}_y) \\ & + \frac{3}{\sqrt{(a^2 + \xi')(b^2 + \xi')}} \left(\frac{d_{0,x} x'}{a^2 + \xi'} + \frac{d_{0,y} y'}{b^2 + \xi'} \right) \\ & \times \left(\frac{P_{xx} x'}{a^2 + \xi'} \mathbf{e}_x + \frac{P_{yy} y'}{b^2 + \xi'} \mathbf{e}_y \right) \left(\frac{x'^2}{(a^2 + \xi')^2} + \frac{y'^2}{(b^2 + \xi')^2} \right)^{-1}, \quad (38) \end{aligned}$$

where the components of the polarizability tensor of an elliptic nanocylinder are:

$$\begin{aligned} P_{xx} &= \frac{1}{3} ab (a + b) \frac{\varepsilon - 1}{a + \varepsilon b}, \\ P_{yy} &= \frac{1}{3} ab (a + b) \frac{\varepsilon - 1}{\varepsilon a + b}, \end{aligned} \quad (39)$$

where ξ' is the positive root of equation $\frac{x'^2}{a^2 + \xi'} + \frac{y'^2}{b^2 + \xi'} = 1$;

$$\begin{aligned} F_a(\xi') &= \frac{2}{\sqrt{a^2 + \xi'} (\sqrt{a^2 + \xi'} + \sqrt{b^2 + \xi'})}, \\ F_b(\xi') &= \frac{2}{\sqrt{b^2 + \xi'} (\sqrt{a^2 + \xi'} + \sqrt{b^2 + \xi'})}. \end{aligned} \quad (40)$$

One can obtain the following expressions for some particular cases of the dipole moment orientation along the Cartesian axes.

A) Dipole moment is oriented along x -axis ($\mathbf{d}_0 = d_0 \mathbf{e}_x$)

$$\begin{aligned} \delta \mathbf{d} = & -\frac{d_0 (\varepsilon - 1) ab (a + b) \mathbf{e}_x}{\sqrt{a^2 + \xi'} (\sqrt{a^2 + \xi'} + \sqrt{b^2 + \xi'}) (a + \varepsilon b)} \\ & + \frac{d_0 (\varepsilon - 1) ab (a + b) x'}{(a^2 + \xi')^{3/2} \sqrt{b^2 + \xi'}} \left(\frac{x'^2}{(a^2 + \xi')^2} + \frac{y'^2}{(b^2 + \xi')^2} \right)^{-1} \\ & \times \left\{ \frac{x' \mathbf{e}_x}{(a^2 + \xi') (a + \varepsilon b)} + \frac{y' \mathbf{e}_y}{(b^2 + \xi') (\varepsilon a + b)} \right\}. \end{aligned} \quad (41)$$

B) Dipole moment is oriented along y -axis ($\mathbf{d}_0 = d_0 \mathbf{e}_y$)

$$\begin{aligned} \delta \mathbf{d} = & - \frac{d_0 (\varepsilon - 1) ab (a + b) \mathbf{e}_y}{\sqrt{b^2 + \xi'} (\sqrt{a^2 + \xi'} + \sqrt{b^2 + \xi'}) (\varepsilon a + b)} \\ & + \frac{d_0 (\varepsilon - 1) ab (a + b) y'}{\sqrt{a^2 + \xi'} (b^2 + \xi')^{3/2}} \left(\frac{x'^2}{(a^2 + \xi')^2} + \frac{y'^2}{(b^2 + \xi')^2} \right)^{-1} \\ & \times \left\{ \frac{x' \mathbf{e}_x}{(a^2 + \xi') (a + \varepsilon b)} + \frac{y' \mathbf{e}_y}{(b + \xi') (\varepsilon a + b)} \right\}. \end{aligned} \quad (42)$$

C) Dipole moment is oriented along z -axis ($\mathbf{d}_0 = d_0 \mathbf{e}_z$)

$$\delta \mathbf{d} = 0 \quad (43)$$

Note that the expressions (41) and (42) in case of circular nanocylinder ($a = b$) are significantly simplified and take the well known form [35]

$$\delta \mathbf{d} = \left(\frac{\varepsilon - 1}{\varepsilon + 1} \right) \left(\frac{a}{\rho'} \right)^2 [-\mathbf{d}_0 + 2 (\mathbf{d}_0 \mathbf{n}') \mathbf{n}'] \quad (44)$$

where $\mathbf{d}_0 = d_{0,x} \mathbf{e}_x + d_{0,y} \mathbf{e}_y$; $\mathbf{n}' = (x' \mathbf{e}_x + y' \mathbf{e}_y) / \rho'$ and $\rho' = \sqrt{x'^2 + y'^2}$.

Because the induced dipole moment (41)-(43) is known, one can find the radiative rate of the spontaneous decay by using Eq.(5). Let an atom be placed on x -axis at point x' . Then it is sufficient to consider two orientations of the dipole moment, in accordance with Eqs. (41)-(43).

A) Dipole moment is oriented along x -axis

$$\left(\frac{\gamma}{\gamma_0} \right)^{radiative} = \left| 1 + \frac{ab(a+b)}{\sqrt{x'^2 - a^2 + b^2} (x' + \sqrt{x'^2 - a^2 + b^2})} \left(\frac{\varepsilon - 1}{a + \varepsilon b} \right) \right|^2. \quad (45)$$

B) Dipole moment is oriented along y -axis

$$\left(\frac{\gamma}{\gamma_0} \right)^{radiative} = \left| 1 - \frac{ab(a+b)}{\sqrt{x'^2 - a^2 + b^2} (x' + \sqrt{x'^2 - a^2 + b^2})} \left(\frac{\varepsilon - 1}{\varepsilon a + b} \right) \right|^2. \quad (46)$$

If the dipole moment of an atom is oriented along the nanocylinder axis (z -axis) then the radiative rate of the spontaneous decay should not be changed.

If an atom is inside a dielectric elliptic cylinder without losses, then the expression for the radiative rate of spontaneous decays will take the following form at arbitrary dipole moment orientation, $\mathbf{d}_0 = d_{0,x} \mathbf{e}_x + d_{0,y} \mathbf{e}_y + d_{0,z} \mathbf{e}_z$,

$$\left(\frac{\gamma}{\gamma_0} \right)^{radiative} = \left(\frac{a+b}{a+\varepsilon b} \right)^2 \frac{d_{0,x}^2}{d_0^2} + \left(\frac{a+b}{\varepsilon a+b} \right)^2 \frac{d_{0,y}^2}{d_0^2} + \frac{d_{0,z}^2}{d_0^2}, \quad (47)$$

which is independent of the atomic position inside the nanocylinder. In deriving (47) we neglect the local field factor [55]. It should be noted that formula (47) is in agreement with that obtained in [56] for the case of two-dimensional ellipse (to obtain that result we must substitute in (47) $d_{0,z} = 0$). It also be noted, that expression (47) can be applied to describe of an atom in elliptic cylindrical cavity in material with permittivity ε_0 . In this case one should make substitution $\varepsilon \rightarrow 1/\varepsilon_0$ and multiply the obtained expression by $\sqrt{\varepsilon_0}$.

Note that Eqs. (45) and (46) have been derived as a limiting case of a finite-size ellipsoid with fixed permittivity. These formulae are unsuitable for describing the radiative decay rate of atoms near conducting (metallic) cylinder, because the waveguided modes (plasmon modes) of the infinite cylinder had not been taken into account. The correct expression for the case of perfectly conducting cylinder is given in Eq.(35).

4.2 The rate of nonradiative decays

In accordance with section 2, the rate of nonradiative decays of an atom near a nanobody is determined by a quasistatic solution of the problem near an elliptic nanocylinder. A Green's function of the Laplace equation expressed in elliptical coordinates may be obtained from the Green's function of the Helmholtz equation (the first terms in the right-hand side of Eqs. (8) and (9)) in the limit $k \rightarrow 0$. As a result of such a procedure in the region $u_0 < u < u'$ the expression for the scalar Green's function may be written in the form

$$\begin{aligned} G_0(\mathbf{r}, \mathbf{r}') &= \frac{1}{|\mathbf{r} - \mathbf{r}'|} \\ &= 4i \sum_{\sigma=e,o} \sum_{n=0}^{\infty} \int_0^{\infty} d\alpha \cos(\alpha(z-z')) \frac{S\sigma_n(i\alpha f, v) S\sigma_n(i\alpha f, v')}{M\sigma_n(i\alpha f)} \\ &\quad \times J\sigma_n(i\alpha f, u) H^{(1)}\sigma_n(i\alpha f, u') \end{aligned} \quad (48)$$

It should be noted here that function $S\sigma_n(i\alpha f, v)$, as follows from (10) and (11), is the real function because the coefficients $B\sigma_n(i\alpha f)$ are real. Functions $J\sigma_n(i\alpha f, u)$ and $H^{(1)}\sigma_n(i\alpha f, u)$ are either real or imaginary depending on the parity of n . The product $J\sigma_n(i\alpha f, u) H^{(1)}\sigma_n(i\alpha f, u')$ is always purely imaginary. Hence, the right-hand side of Eq.(48) is the real function.

Using Eq.(48) one can obtain a quasistatic solution for the potential of a dielectric nanocylinder, with dielectric constant ε , excited by the point-like dipole source located at the point with (u', v', z) coordinates. The solution for the potential ϕ^r induced in space near the cylinder has the form:

$$\begin{aligned} \phi^r &= 4i(\mathbf{d}_0 \nabla') \sum_{\sigma=e,o} \sum_{n=0}^{\infty} \int_0^{\infty} d\alpha \cos(\alpha(z-z')) \frac{S\sigma_n(i\alpha f, v) S\sigma_n(i\alpha f, v')}{M\sigma_n(i\alpha f)} \\ &\quad \times H^{(1)}\sigma_n(i\alpha f, u) H^{(1)}\sigma_n(i\alpha f, u') A\sigma_n(i\alpha f, u_0), \end{aligned} \quad (49)$$

where the elliptical wave reflection coefficient has the form

$$\begin{aligned}
A\sigma_n(s, u_0) &= (\varepsilon - 1) \frac{\partial}{\partial w} J\sigma_n(s, w) \Big|_{w=u_0} J\sigma_n(s, u_0) \\
&\times \left\{ \frac{\partial}{\partial w} H^{(1)}\sigma_n(s, w) \Big|_{w=u_0} J\sigma_n(s, u_0) \right. \\
&\left. - \varepsilon \frac{\partial}{\partial w} J\sigma_n(s, w) \Big|_{w=u_0} H^{(1)}\sigma_n(s, u_0) \right\}^{-1}. \quad (50)
\end{aligned}$$

For metallic elliptic cylinders with low losses ($\varepsilon = \varepsilon' + i\varepsilon''$; $\varepsilon' < 0$, $\varepsilon'' \ll |\varepsilon'|$) denominator of (50) becomes close to zero for some longitudinal wavenumbers (plasmon modes). In this case quasistatic approximation is not valid and one should use full set of Maxwell's equations. In the case of elliptic nanocylinder made of real metals ($\varepsilon = \varepsilon' + i\varepsilon''$, $\varepsilon'' \sim 1$) or dielectrics the denominator of (50) is always nonzero and quasistatic approximation is valid in this case. So we restrict ourselves for the case of dielectric elliptic nanocylinders made of real metals or dielectrics.

By calculating the reflected field $\mathbf{E}^r = -\nabla\phi^r$ with the help of (49) and using (2) and (4) we obtain the following expressions for the quasistatic contribution to the nonradiative rate of the spontaneous decay of an atom near the dielectric (metallic) nanocylinder.

Dipole moment is oriented along x-axis ($\mathbf{d}_0 = d_0\mathbf{e}_x$)

$$\begin{aligned}
\left(\frac{\gamma}{\gamma_0}\right)_x^{nonrad} &= -\frac{6}{k^3 f^2} \sum_{\sigma=e,o} \sum_{n=0}^{\infty} \int_0^{\infty} d\alpha \frac{[S\sigma_n(i\alpha f, v')]^2}{M\sigma_n(i\alpha f)} [H^{(1)}\sigma_n(i\alpha f, u')]^2 \\
&\times \left\{ v' \left(\frac{u'^2 - 1}{u'^2 - v'^2} \right) \frac{(\partial/\partial w) H^{(1)}\sigma_n(i\alpha f, w)|_{w=u'}}{H^{(1)}\sigma_n(i\alpha f, u')} \right. \\
&\left. + u' \left(\frac{1 - v'^2}{u'^2 - v'^2} \right) \frac{(\partial/\partial w) S\sigma_n(i\alpha f, w)|_{w=v'}}{S\sigma_n(i\alpha f, v')} \right\}^2 \\
&\times \text{Re}[A\sigma_n(i\alpha f, u_0)]. \quad (51)
\end{aligned}$$

Dipole moment is oriented along y-axis ($\mathbf{d}_0 = d_0\mathbf{e}_y$)

$$\begin{aligned}
\left(\frac{\gamma}{\gamma_0}\right)_y^{nonrad} &= -\frac{6(u'^2 - 1)(1 - v'^2)}{k^3 f^2 (u'^2 - v'^2)^2} \sum_{\sigma=e,o} \sum_{n=0}^{\infty} \int_0^{\infty} d\alpha \frac{[S\sigma_n(i\alpha f, v')]^2}{M\sigma_n(i\alpha f)} \\
&\times [H^{(1)}\sigma_n(i\alpha f, u')]^2 \left\{ u' \frac{(\partial/\partial w) H^{(1)}\sigma_n(i\alpha f, w)|_{w=u'}}{H^{(1)}\sigma_n(i\alpha f, u')} \right. \\
&\left. - v' \frac{(\partial/\partial w) S\sigma_n(i\alpha f, w)|_{w=v'}}{S\sigma_n(i\alpha f, v')} \right\}^2 \text{Re}[A\sigma_n(i\alpha f, u_0)]. \quad (52)
\end{aligned}$$

Dipole moment is oriented along z -axis ($\mathbf{d}_0 = d_0 \mathbf{e}_z$)

$$\begin{aligned} \left(\frac{\gamma}{\gamma_0}\right)_z^{nonrad} &= -\frac{6}{k^3} \sum_{\sigma=e,o} \sum_{n=0}^{\infty} \int_0^{\infty} d\alpha \alpha^2 \frac{[S\sigma_n(i\alpha f, v')]^2}{M\sigma_n(i\alpha f)} \\ &\quad - \frac{6}{k^3} \sum_{\sigma=e,o} \sum_{n=0}^{\infty} \int_0^{\infty} d\alpha \alpha^2 \frac{[S\sigma_n(i\alpha f, v')]^2}{M\sigma_n(i\alpha f)}. \end{aligned} \quad (53)$$

If an atom is placed very close to the nanocylinder the nonradiative spontaneous decay rate may be approximated by the expressions, which describe nonradiative processes near a plane surface [58]. For dipole with tangential and normal to surface of cylinder orientations we have respectively

$$\begin{aligned} \left(\frac{\gamma}{\gamma_0}\right)_{tang}^{nonrad} &= \frac{3}{16(k\Delta')^3} \text{Im} \left(\frac{\varepsilon - 1}{\varepsilon + 1} \right), \\ \left(\frac{\gamma}{\gamma_0}\right)_{norm}^{nonrad} &= 2 \left(\frac{\gamma}{\gamma_0}\right)_{tang}^{nonrad}. \end{aligned} \quad (54)$$

Here Δ' is the distance from atom to surface; in the case of an elliptic cylinder we can write $\Delta' = \zeta' \sqrt{\frac{x'^2}{(\zeta'+a^2)^2} + \frac{y'^2}{(\zeta'+b^2)^2}}$, where ζ' is the positive root of the equation $\frac{x'^2 a^2}{(\zeta'+a^2)^2} + \frac{y'^2 b^2}{(\zeta'+b^2)^2} = 1$.

5 Graphic illustrations and discussion of results

Let us first consider an atom near a dielectric nanocylinder. Figure 4 illustrates the radiative rate of the spontaneous decay (45) and (46) near the dielectric nanocylinder. As an atom moves away from the surface the decay rate tends to the value, which corresponds to the case of an atom in free space in the absence of a nanobody. As the dielectric constant of the nanocylinder material is increased, the radiative rate for the normally oriented dipole moment of an atom increases by tending to large (finite) value, and for the tangentially oriented dipole moment it decreases by tending to low values (zero). The most increase in the decay rate occurs for the normally-oriented atom in the direction of the larger semi-axis (Fig.4(a)).

From Fig.5 it is seen how the decay rate changes for an atom located in close proximity to the surface of a nanocylinder depending on the ratio between the a and b elliptic semi-axes. If one of the nanocylinder semi-axes tends to zero (the case of a dielectric nanobelt) then from (45) and (46) it follows that $\gamma^{radiative}/\gamma_0 \rightarrow \varepsilon^2$ for the normally-oriented dipole moment of an atom placed at the belt edge, while for the tangential orientation of the dipole moment we obtain $\gamma^{radiative}/\gamma_0 \rightarrow 1/\varepsilon^2$ (Fig.5(a)). For the atom placed at the belt facet,

independent of the dipole moment orientation, we obtain $\gamma^{radiative}/\gamma_0 \rightarrow 1$ (Fig.5(b)).

Figure 6 illustrates radiative and nonradiative rates of the spontaneous decay as the function of the distance of an atom to the surface of the dielectric elliptic nanocylinder having the permittivity $\varepsilon = 3 + i10^{-8}$. The atom is shifted along the x -axis and its dipole moment is oriented along this axis. To calculate the Mathieu functions we have used of the method [59] based on the solution of the generalized eigen-value problem for the coefficients $B\sigma_n^m$. The integration of (51)-(53) was performed by the mean-value method using the Aitken's process [60] for acceleration of the integral convergence. As seen from Fig.6 the radiative rate of the spontaneous decay for a dielectric with a very small imaginary part of permittivity is dominating, as a whole, over a nonradiative rate, and takes maximal values at the cylinder surface. But if the atom is placed very close to the nanocylinder surface, the nonradiative rate exceeds over the radiative one, and at $u' = u_0$ it turns to the infinity, as follows from the asymptotic expression (54) depicted by dotted line in Fig. 6. Let us determine the distance, on which the radiative and nonradiative rates for the normally oriented dipole moment of an atom coincide. By equating (45) with (54), for the case of a small imaginary part of the permittivity $\varepsilon = \varepsilon' + i\varepsilon''$ of a cylinder ($\varepsilon'' \ll \varepsilon'$), we get that at

$$\frac{x' - a}{a} \approx \frac{1}{ka} \left\{ \frac{3}{4} \frac{\varepsilon''}{(1 + \varepsilon')^2} \frac{(a + \varepsilon'b)^2}{\varepsilon'^2 (a + b)^2} \right\}^{1/3} \quad (55)$$

the nonradiative contribution to decay rate is equal to the radiative one. For the case represented in Fig.6 we obtain: $(x' - a)/a \approx 4.4 \times 10^{-3}$, which means that one may actually neglect here the nonradiative processes. If the atom is y -shifted and has the dipole moment oriented along this axis, then from (55) we obtain

$$\frac{y' - b}{a} \approx \frac{1}{ka} \left\{ \frac{3}{4} \frac{\varepsilon''}{(\varepsilon' + 1)^2} \frac{(\varepsilon'a + b)^2}{\varepsilon'^2 (a + b)^2} \right\}^{1/3}. \quad (56)$$

Figure 7 illustrates decay rates for a silver nanocylinder with $\varepsilon = -3.02 + i0.21$ ($\lambda = 373$ nm [61]). The ratio of the elliptical semi-axes is $a/b=3$ and $a=6$ nm ($ka \approx 0.1$). As is well seen, the region nearby cylinder, where the nonradiative rate is greater than radiative, is essentially wider than the region represented in Fig.6. This is due to a larger imaginary part of permittivity of the nanocylinder material. At small distances from the cylinder surface the nonradiative rate of the spontaneous decay increases in accordance with (54) (dotted line of Fig.7), and at large distances from the cylinder surface, it tends to zero.

Now let us consider the case of a perfectly conducting cylinder. The integration of Eqs. (17)-(26) was performed by the method of mean values with using the Aitken's process. Figure 8 illustrates the spontaneous decay rate of an atom placed near a perfectly conducting elliptic cylinder ($ka = 1$), as the function of the atom's position along the larger semi-axis a . As is seen, the decay rate

achieves the maximum in close proximity to the cylinder surface ($u' = u_0$) for the normally oriented dipole moment of an atom (x-line of Fig.7(a) or y-line of Fig.8(b)). For the tangentially oriented dipole moment we obtain zero at the surface of the cylinder (y-line of Fig.8(a) or x-line of Fig.8(b), and also z-line) resulting from a full compensation of the dipole moment of an atom. As the ratio of semi-axes increases (when the smaller semi-axis b decreases) the maximum rate of the spontaneous decay is increased (cf. x-lines in Fig.8(a) and Fig.8(b)) and tends to infinitely large values in the limit of $b \rightarrow 0$, which agrees with the asymptotic formula (35) for the nanocylinder.

Figure 9 illustrates the spontaneous decay rate of an atom placed near a perfectly conducting elliptic cylinder ($ka = 1$) as the function of the atomic displacement along y-axis (towards a smaller semi-axis). The decay rate achieves the maximal value (normal orientation of the dipole moment) and the minimal value (tangential orientation) at the surface of a cylinder. At high values of the semi-axes ratio, the curves y and z (Fig.9(b) for $a/b = 100 \gg 1$) look like the well known solutions [58] for the spontaneous decay rate of an atom near a perfectly conducting plane surface with the normal (curve y) and tangential (curve z) orientations of the dipole moment. The maximum value of the decay rate here is about 2. The behavior of decay rate of an atom with x orientation of dipole momentum is slightly different from the case of the plane mirror because of edge effects in case of strip.

Figure 10 illustrates the decay rate of an atom placed in close proximity to the surface of a perfectly conducting cylinder ($u' = u_0$). The dipole moment is oriented normally to the cylinder surface along the larger semi-axis (Fig.10(a)) and along the smaller semi-axis (Fig.10(b)). As seen from Fig.10, the expression (35) obtained in the case of $ka \rightarrow 0$ for the atom with normal orientation, tends to infinitely large values, which disagrees with the finite values derived from the quasistatic expression (45) in the limit of $\varepsilon \rightarrow \infty$. This difference follows from the fact that the amplitude of the surface current propagating along the cylinder at $ka \rightarrow 0$ increases infinitely large [26]. In other words, perfectly conducting cylinder of infinitely small cross-section is a kind of antenna, which is effectively excited by a point dipole (atom). This means that the induced dipole moment of the perfectly conducting cylinder and the rate of spontaneous decay of an atom also tend to infinity at $ka \rightarrow 0$ (see Eq.(36)). The analogous process is also observed in the case of a circular nanocylinder (dotted line in Fig.10, Eq.(37)).

Figure 11 illustrates a comparison for the rate of spontaneous decay (16) obtained by numerical integration (34) and an asymptotic expression (35) for the atom with the normally oriented dipole moment in close proximity to the surface ($u' = u_0$) of perfectly conducting cylinder. As it seen, the asymptotic expression agrees well with the numerical data up to $ka = 1$. It can, therefore, be suitable for a fast evaluation of the spontaneous decay rate near the nanocylinder and for verification of the numerical solution.

6 Conclusion

Thus, in this paper we obtained the analytical expressions for the radiative rate of the spontaneous decay of an atom near a dielectric nanocylinder of elliptical cross-section within the framework of a quasistatic approximation. The retardation effects are taken into account for the spontaneous decay of an atom near a perfectly conducting elliptic cylinder, where the analytical solution can be found at arbitrary parameters of the problem. Special attention is paid to the case of a nanocylinder where the largest semi-axis of the cylinder is much less than wavelength. It is shown that a decrease in the cross-section of a metallic (perfectly conducting) nanocylinder leads to an infinite increase in the spontaneous decay rate for a normally oriented dipole moment of the atom. A simple asymptotic expression for the spontaneous decay rate has been obtained in the case of a perfectly conducting nanocylinder. For the atom placed in close proximity to a belt edge one can obtain arbitrary large values of the decay rate by means of tuning elliptic semi-axes. The obtained results can be used for checking the numerical solution in a more complex case of the dielectric elliptic cylinder. The results of this work may be also helpful at studying an interaction of atoms (molecules) with nanobelts and nanoribbons.

Acknowledgement. The authors are grateful to the Russian Fund of Fundamental Studies (grants 05-02-19647 and 07-02-01328) and the RAS Presidium Program “The effect of atomic-crystalline and electron structures on properties of the condensed media” for a partial financial support of the present work.

One of the authors (D.V.G.) is thankful to the Young scientists support Program of the Educational-Scientific Center of P.N. Lebedev Physical Institute and the RAS Presidium Program “Support of young scientists” for a partial financial support of the present work.

References

- [1] E.M. Purcell, Phys. Rev. **69**, 681 (1946).
- [2] *Cavity Quantum Electrodynamics*, P. Berman (ed.) (Academic, New York, 1994).
- [3] Zh.I. Alferov, Rev. Mod. Phys. **73**, 767 (2001).
- [4] P.N. Prasad, *Introduction to Nanophotonics* (Wiley-Interscience, New York, 2004).
- [5] H. Chew J. Chem. Phys. **87**, 1355 (1987).
- [6] V.V. Klimov, M. Ducloy, and V.S. Letokhov, J. Modern Optics **43**, 2251 (1996).
- [7] V.V. Klimov and V.S. Letokhov, Laser Phys. **15**, 61 (2005).

- [8] V.V. Klimov, M. Ducloy, and V.S. Letokhov, Eur. Phys. J. D **20**, 133 (2002).
- [9] D.-S. Wang and M. Kerker, Phys. Rev. B **24**, 1777 (1981).
- [10] J. Gersten, A. Nitzan, J. Chem. Phys. **75**, 1139 (1981).
- [11] D.V. Guzatov, V.V. Klimov, Chem. Phys. Lett. **412**, 341 (2005).
- [12] J. Denschlag, G. Umshaus, J. Schmiedmayer, Phys. Rev. Lett. **81**, 737 (1998).
- [13] J. Denschlag, D.Cassetari, A. Chenet, S. Schneider, J. Schmiedmayer, Appl. Phys. B **69**, 291 (1999).
- [14] W.A. Lyon, S.M. Nie, Anal. Chem. **69**, 3400 (1997).
- [15] C. Zander, K.H. Drexhage, K.T. Han, J. Wolfrum, M. Sauer, Chem. Phys. Lett. **286**, 457 (1998).
- [16] D.Y. Chu, S.T. Ho, J. Opt. Soc. Am. B **10**, 381 (1993).
- [17] D.Y. Chu, S.T. Ho, J.P. Zhang and M.K. Chin, in: *Optical Processes in Microcavities*, R.K. Chang, A.J. Campillo (eds.) (World Scientific, Singapore, 1996).
- [18] X. Duan, Y. Huang, R. Agarwal and C. M. Lieber, Nature **421**, 241 (2003).
- [19] J. C. Johnson, H.-J. Choi, K. P. Knutsen, R. D. Schaller, P. Yang and R. J. Saykally, Nature Materials **1**, 106110 (2002).
- [20] C. Dekker, Physics Today **52**, 22 (1999).
- [21] R. Saito, G. Dresselhaus, M.S. Dresselhaus, *Physical Properties of Carbon Nanotubes* (Imperial College Press, London, 1998).
- [22] S.D. Brorson, H. Yokoyama and E.P. Ippen, IEEE J. Quant. Electronics **26**, 1492 (1990).
- [23] S.D. Brorson, P.M.W. Skovgaard, in: *Optical Processes in Microcavities*, R.K. Chang, A.J. Campillo (eds.) (World Scientific, Singapore, 1996).
- [24] M.A. Rippin, P.L. Knight, J. Mod. Optics **43**, 807 (1996).
- [25] K. Kakazu and Y.S. Kim, Progress Theor. Phys. **96**, 883 (1996).
- [26] V.V. Klimov, M.Ducloy, Phys. Rev. A **62**, 043818 (2000).
- [27] K. Oshiro and K. Kakazu, Progress Theor. Phys. **98**, 883 (1997).
- [28] M. Boustimi, J. Baudon, P. Candori, and J. Robert, Phys. Rev. B **65**, 155402 (2002).

- [29] B.Z. Katsenelenbaum, Zhurnal Tekhnicheskoi Fiziki [in Russian] **XIX**, 1168 (1949).
- [30] B.Z. Katsenelenbaum, Zhurnal Tekhnicheskoi Fiziki [in Russian] **XIX**, 1182 (1949).
- [31] H. Nha, W. Jhe, Phys. Rev. A **56**, 2213 (1997).
- [32] J. Enderlein, Chem. Phys. Lett. **301**, 430 (1999).
- [33] W. Zakowicz, M. Janowicz, Phys. Rev. A **62**, 013820 (2000).
- [34] T. Sondergaard and B. Tromborg, Phys. Rev. A **64**, 033812 (2001).
- [35] V.V. Klimov, M. Ducloy, Phys. Rev. A **69**, 013812 (2004).
- [36] Fam Le Kien, S. Dutta Gupta, V.I. Balykin, and K. Hakuta, Phys. Rev. A **72**, 032509 (2005).
- [37] S.A. Maksimenko, G.Ya. Slepyan, Radiotekhnika i Elektronika [in Russian] **47**, 261 (2002).
- [38] I.V. Bondarev, S.A. Maksimenko, G.Ya. Slepyan, Phys. Rev. Lett. **89**, 115504 (2002).
- [39] Z.W. Pan, Z.R. Dai and Z.L. Wang, Science **291**, 1947 (2001).
- [40] C. Ma, D. Moore, J. Li and Z. L. Wang, Adv. Mater. **15**, 228 (2003).
- [41] Z.L. Wang, Adv. Mater. **15** 432 (2003).
- [42] Z.R. Dai, Z.W. Pan and Z.L. Wang, J. Phys. Chem. B **106**, 902 (2002).
- [43] W.-Q. Han, L. Wu, Y. Zhu, and M. Strongin, Nano Lett. **5**, 1419 (2005).
- [44] X.Y. Kong and Z.L. Wang, Nano Lett. **2**, 1625 (2003).
- [45] Z.L. Wang, X.Y. Kong and J.M. Zuo, Phys. Rev. Lett. **91**, 185502 (2003).
- [46] *Nanowires and Nanobelts – materials, properties and devices*, Zh.L. Wang (ed.) (Kluwer Academic Publisher, 2003).
- [47] X.Y. Kong, Y. Ding, R.S. Yang, Z.L. Wang, Science **303**, 1348 (2004).
- [48] P.M. Morse and H. Feshbah, *Methods of Theoretical Physics* (McGraw-Hill, New York, 1953).
- [49] J.M. Wylie, and J.E. Sipe, Phys. Rev. A **30**, 1185 (1984).
- [50] A.F. Stevenson, Appl. Phys. **24**, 1134 (1953).
- [51] W.S. Lucke, Appl. Phys. **22**, 14 (1951).

- [52] P.L.E. Uslenghi and N.R. Zitron, in: *Electromagnetic and Acoustic Scattering by Simple Shapes* (North-Holland, Amsterdam, 1969).
- [53] J.A. Stratton, *Electromagnetic Theory* (McGraw-Hills, New York, 1941).
- [54] L.-W. Li, H.-G. Wee, and M.-S. Leong, *IEEE Trans. Antenn. Propagat.* **51**, 564 (2003).
- [55] R.J. Glauber, M. Lewenstein, *Phys. Rev. A* **43**, 467 (1991).
- [56] L. Rogobete, C. Henkel, *Phys. Rev. A* **70**, 063815 (2004).
- [57] W.R. Smythe, *Static and Dynamic Electricity* (McGraw-Hill, New York, 1950).
- [58] R.R. Chance, A. Prock and R. Sylbey, in: *Advances in chemical physics*, I. Prigogine, S.A. Rice (eds.) (John Wiley & Sons, New York, 1978).
- [59] J.J. Stamnes and B. Spjelkavik, *Pure Appl. Opt.* **4**, 251 (1995).
- [60] N.N. Kalitkin, *Numerical Methods* [in Russian] (Nauka, Moscow, 1978).
- [61] P.B. Johnson and R.W. Christy, *Phys. Rev. B* **6**, 4370 (1972).

List of Figure Captions

Fig.1 The nanobelts [39].

Fig.2 Geometry of the problem.

Fig.3 Elliptic cylinder coordinate system.

Fig.4 Radiative decay rate of an atom near a dielectric elliptic nanocylinder as the function of the position of an atom. (a) atom is shifted along x -axis; (b) atom is shifted along y -axis. Dipole moment orientation: x - along x -axis; y - along y -axis. Solid line corresponds to $\varepsilon = 3$; dotted line corresponds to $\varepsilon = 10$. Nanocylinder semi-axes ratio $a/b = 5$.

Fig.5 Radiative decay rate of an atom near the surface of a dielectric ($\varepsilon = 3$) elliptic nanocylinder as the function of the semi-axes ratio for the atom in close proximity to the surface of the nanocylinder. (a) atom is placed on x -axis at point $x' = a$; (b) atom is placed on y -axis at point $y' = a$. Dipole moment orientation: x - along x -axis; y - along y -axis.

Fig.6 Radiative and nonradiative decay rates of an atom as the functions of its position relative to a dielectric elliptic nanocylinder with permittivity $\varepsilon = 3 + i10^{-8}$. The ratio of the nanocylinder semi-axes $a/b = 6$; $ka = 0.1$. The atom is shifted by x -axis with the dipole moment oriented along this axis. The dotted line corresponds to the asymptotic form (54).

Fig.7 Radiative and nonradiative decay rates of an atom as the functions of its position relative to the silver elliptic nanocylinder with permittivity $\varepsilon = -3.02 + i0.21$ ($\lambda = 373$ nm [61]). The atom is shifted by x -axis with the dipole moment oriented along this axis. The ratio of the nanocylinder semi-axes is $a/b = 3$; $a = 6$ nm. The dotted line corresponds to the asymptotic form (54).

Fig.8 Decay rate of an atom placed near a perfectly conducting elliptic cylinder ($ka = 1$) as the function of atom's position relative to the cylinder. The atom is shifted along the x -axis. Dipole moment orientation: x - along x -axis; y - along y -axis; z - along z -axis. The semi-axes ratio: (a) $a/b = 3$; (b) $a/b = 10$.

Fig.9 Decay rate of an atom placed near a perfectly conducting elliptic cylinder ($ka = 1$) as the function of atom's position relative to the cylinder. The atom is shifted along the y -axis. Dipole moment orientation: x - along x -axis; y - along y -axis; z - along z -axis. The semi-axes ratio: (a) $a/b = 3$; (b) $a/b = 100$.

Fig.10 Decay rate of an atom placed in close proximity to the surface of a perfectly conducting elliptic cylinder ($u' = u_0$), as the function of ka . The ratio of the cylinder semi-axes: 1 - $a/b = 3$; 2 - $a/b = 10$; 3 - $a/b = 100$. The dotted line corresponds to the case of $a/b = 1$. (a) atom is located on x -axis at point $x = x'$, and its dipole moment is oriented along x -axis; (b) atom is located on y -axis at point $y = y'$, and its dipole moment is oriented along y -axis.

Fig.11 A comparison of an asymptotic expression for the spontaneous decay rate (35) with (16) obtained by numerical integration of (34) for the atom with the normal dipole moment orientation placed in close proximity to the perfectly conducting cylinder surface ($u' = u_0$). A solid line corresponds to a numerical solution; the crosses denote asymptotic expression. The ratio of semi-axes: 1 -

$a/b = 3$ and $2 - a/b = 1$. Position of an atom relative to the cylinder surface is marked by arrow.

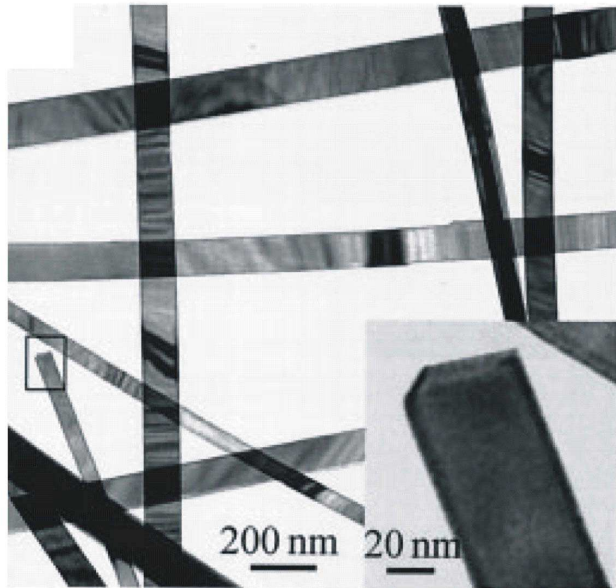
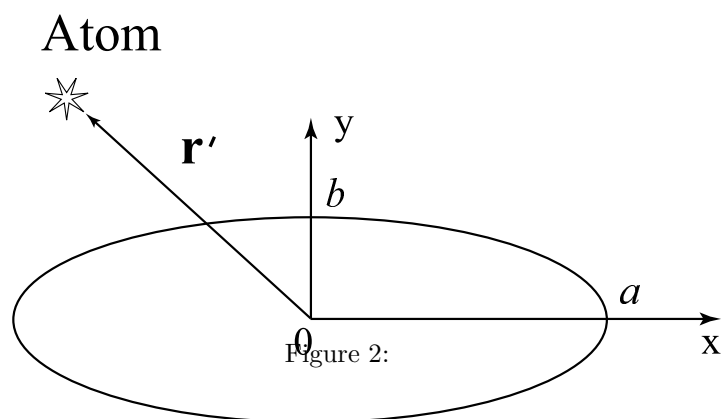


Figure 1:



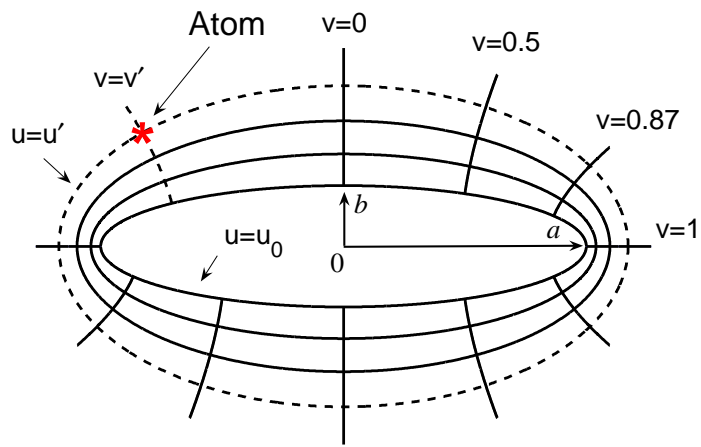


Figure 3:

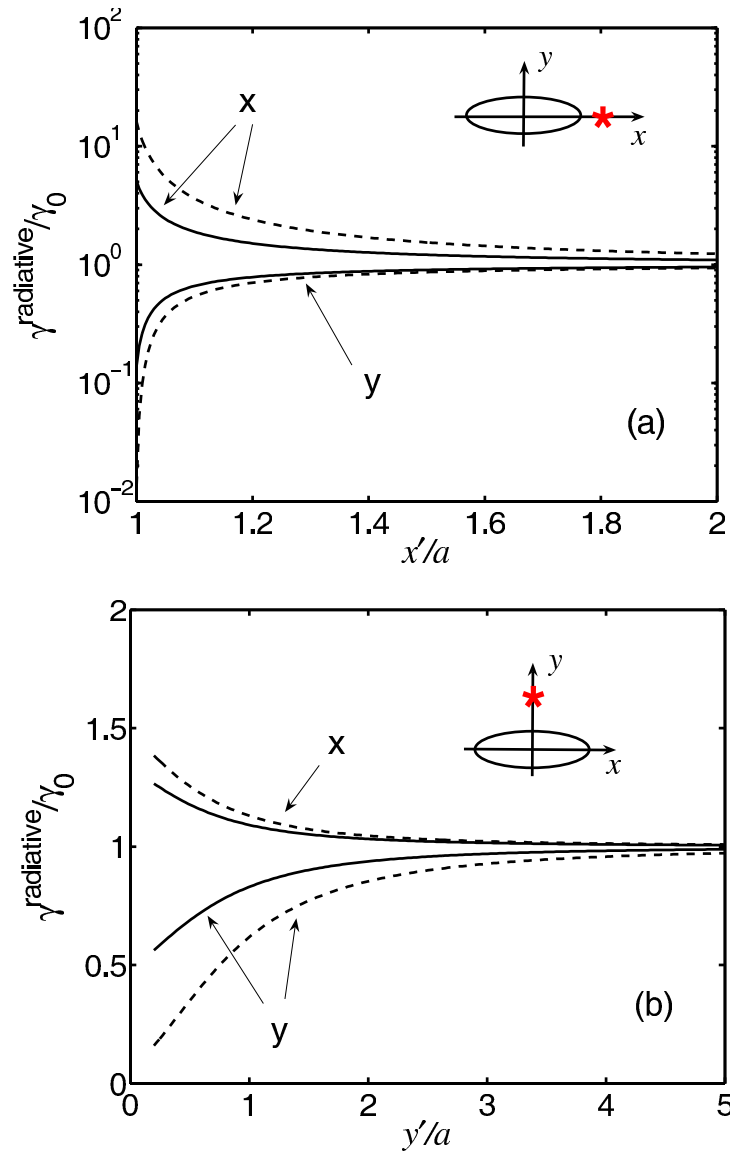


Figure 4:

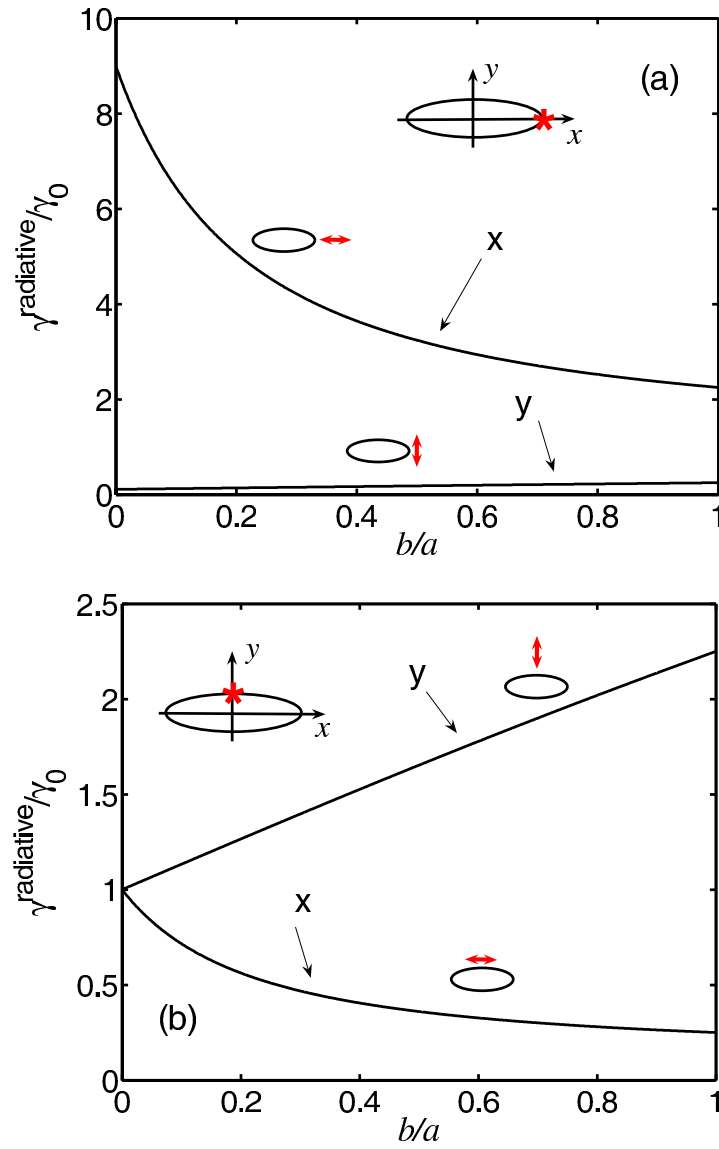


Figure 5:

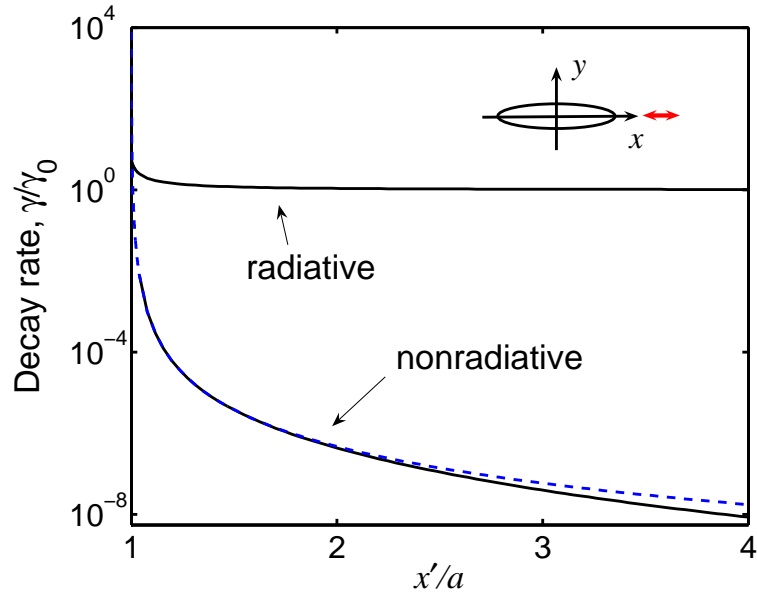


Figure 6:

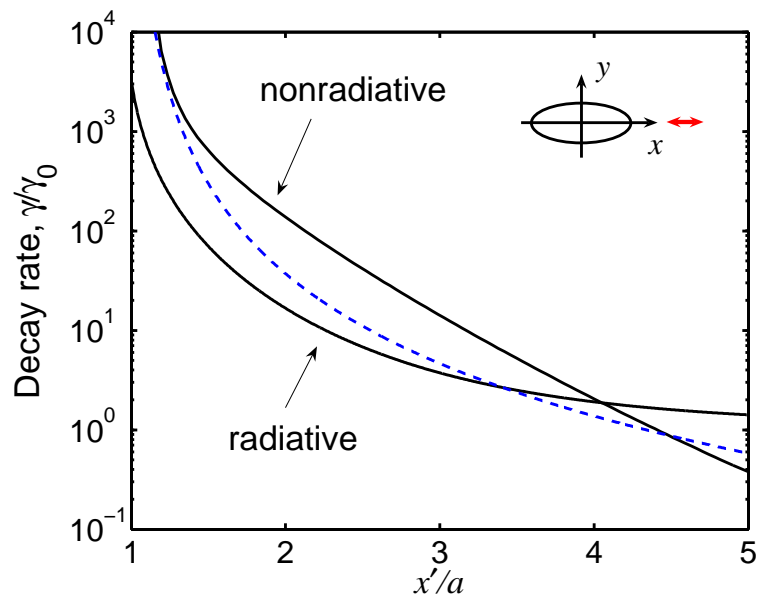


Figure 7:

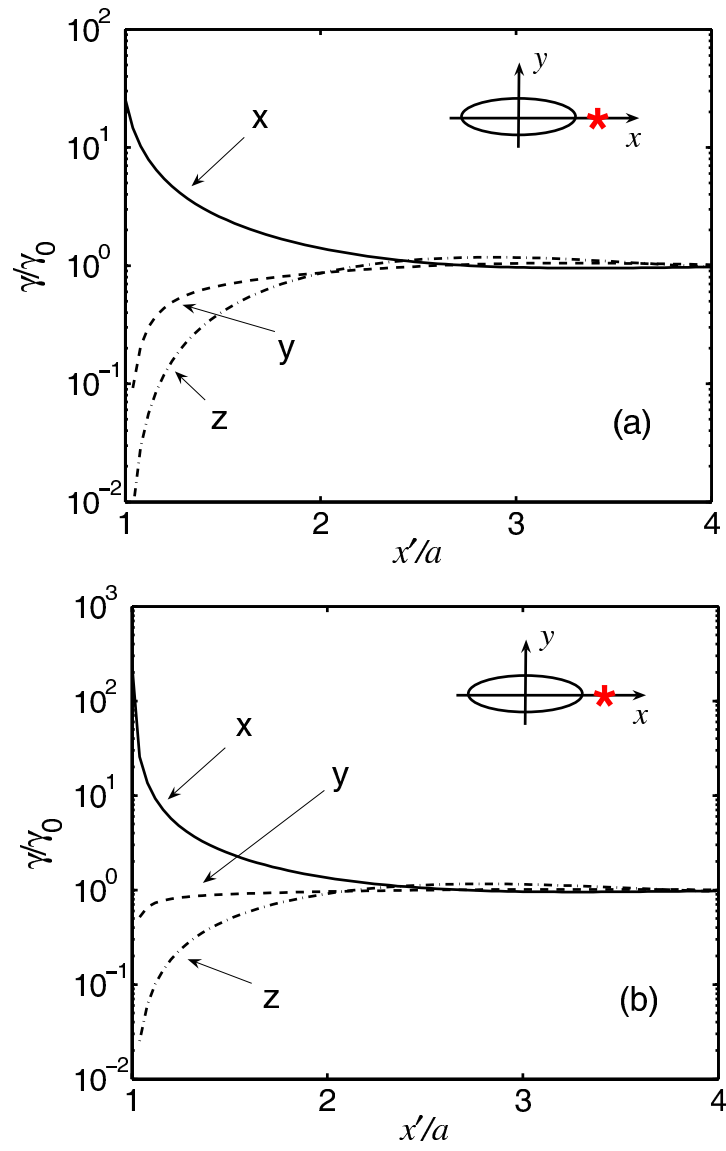


Figure 8:

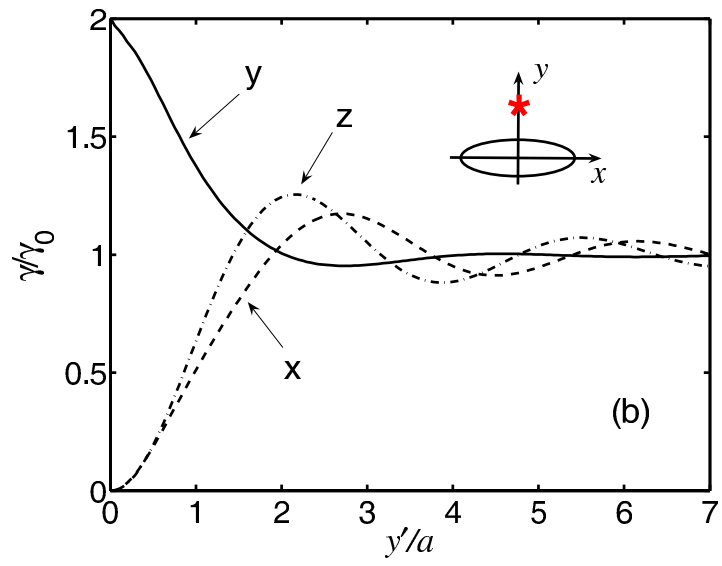
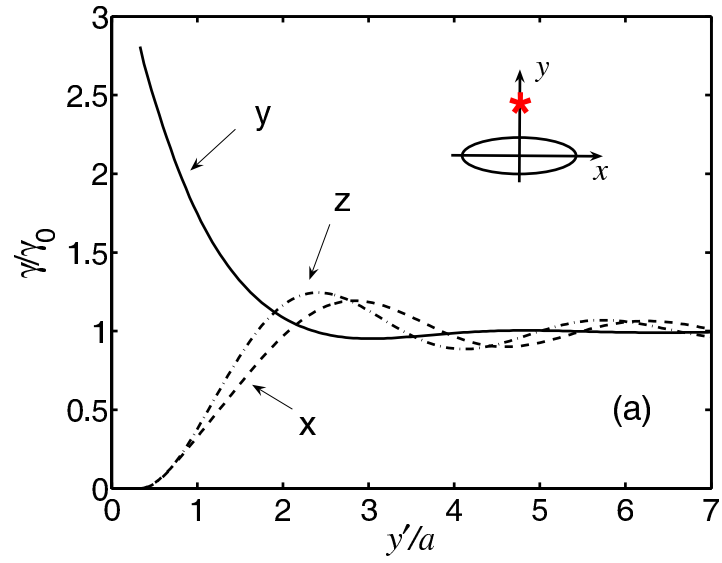


Figure 9:

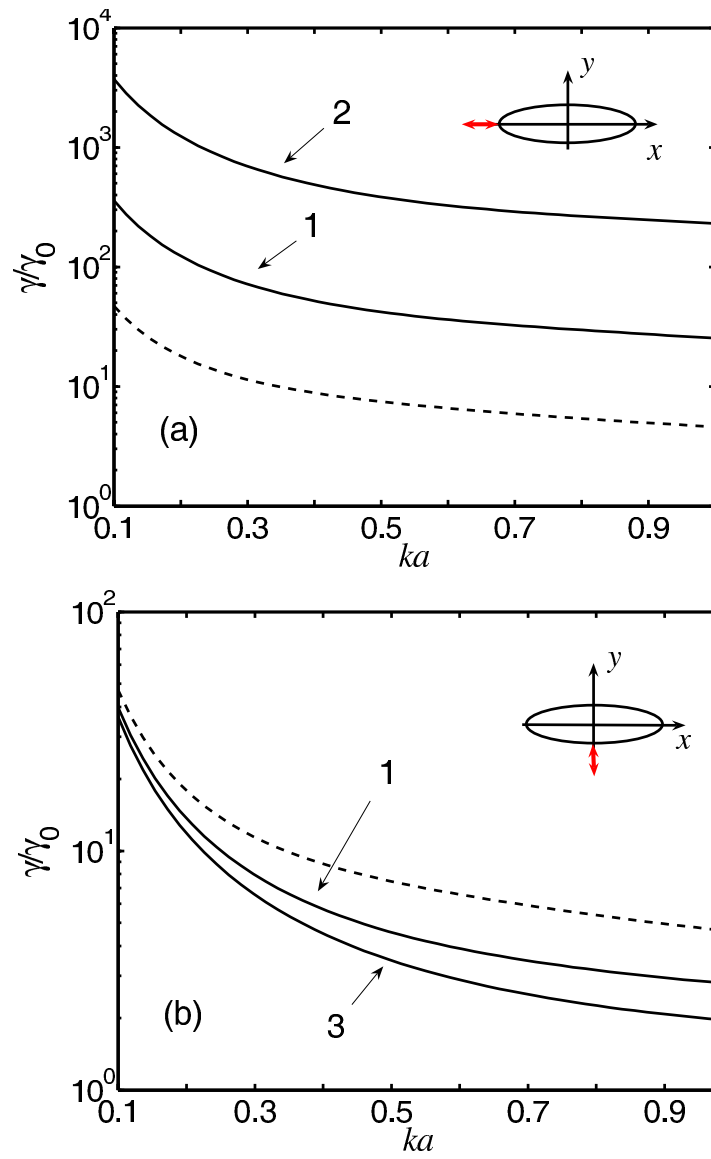


Figure 10:

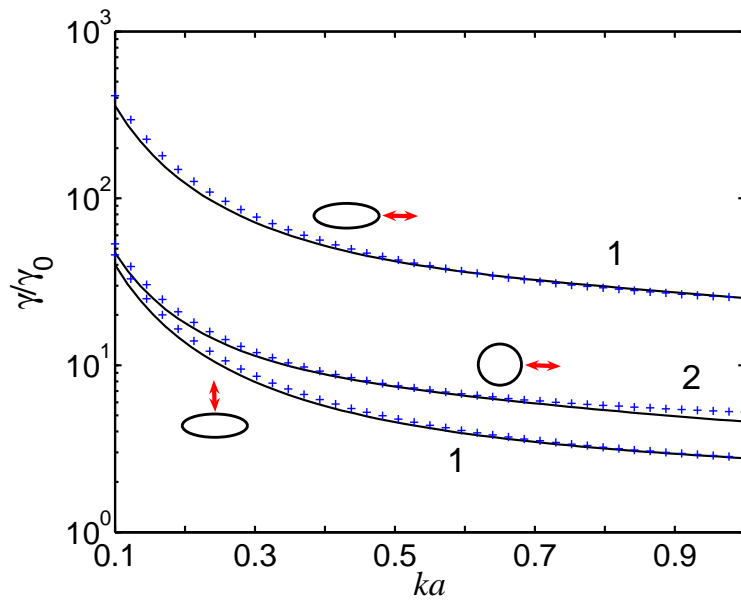


Figure 11: